LAWRENCE
LIVERMORE
NATIONAL
LABORATORY

Behavior of Explosives Under Pressure in a Diamond Anvil Cell

M. F. Foltz

August 23, 2006

Disclaimer

BEHAVIOR OF EXPLOSIVES UNDER PRESSURE

IN A DIAMOND ANVIL CELL

M. Frances Foltz[*]

[*]Lawrence Livermore National Laboratory, Livermore, CA 94551

ABSTRACT

Diamond anvil cell (DAC) studies are used to study the pressure dependence of materials and reactions under conditions comparable to shock loading. We discuss observed DAC pressure-induced changes of Triaminotrinitrobenzene (TATB), Nitromethane (NM), and Hexanitrohexaazaisowurtzitane (CL-20 or HNIW). The NM burn rate, a near monotonic increase up to a peak~30 GPa, is used as baseline behavior since the other explosives are far more complex. TATB samples developed shiny (metallic) polycrystalline zones surrounded by a gradation of color (red to yellow) along the radial pressure gradient. Color changes are believed due to disturbances in the electronic resonance structure as the intermolecular distance decreases. The four polymorphs of CL-20 (α, β, γ, $\tilde{\varepsilon}$-) remain clear up to ~30 GPa. One polymorph (β) was highly sensitive to laser light in a narrow pressure range. While each polymorph has a distinct pressure-dependent burn rate, the similarities yield clues about polymorphic phase transitions.

INTRODUCTION

After decades of study, the complex role that explosive chemistry plays in driving combustion and detonation reaction processes is still not fully understood. This lack of

understanding hinders development of accurate predictive codes. To this end scientists continue to study the relationship between the detonation properties of high explosives (HE) under dynamic conditions to behavior observed under static high pressure. Observations across the entire detonation process need to be reconciled, from nascent initiation phenomena and evolution of exothermic/endothermic processes, to the generation of reaction products behind the shock or combustion front. As part of this effort, diamond anvil cell (DAC) studies look at the pressure dependence of material properties and reactions.

Our previously published diamond anvil cell (DAC) work described burn rate as a function of pressure for several energetic molecules: nitromethane (NM),[1] Triaminotrinitrobenzene (TATB),[2] pentaerythritol-tetranitrate (PETN),[3] ammonium perchlorate (AP),[4] and hexanitrohexaazaisowurtzitane (HNIW, or CL–20).[5] Both the PETN and CL-20 studies included static-pressure mid-infrared FTIR spectra. Here we relate additional qualitative information collected for TATB, Nitromethane, and CL-20 to provide calibration markers for current modeling efforts.

EXPERIMENTAL DETAILS

Details concerning the Bassett-type DAC and instrumentation used to measure pressure and burn rates have been described in earlier work.[1-5] We applied pressures up to ~40 GPa to NM and TATB, and up to ~30 GPa to the four polymorphs of CL-20 (α, β, γ, ε). For all materials studied but TATB, the imaging Argon ion laser beam was transmitted through the sample. Due to the opacity of the TATB, the laser light was reflected from the ignition plane of the sample into the camera focusing optics. In addition, we took several

still photos of TATB samples under pressure and of residue under pressure after removal from the DAC. These photos document interesting visual effects that were only briefly mentioned in Reference 2. No other color changes were seen in any of the other energetic materials studied, including unpublished work on β-HMX (Octogen) and the liquid energetic explosive bis(2-fluoro-2,2-dinitroethyl) formal (FEFO).

In many high-pressure studies the pressure gradient across the sample is minimized to create a homogenous medium for accurately locating phase transitions. In order to do this, the sample diameter is small to minimize the effect of the pressure gradient. To reach high pressures (30-40 GPa), however, it may be necessary to use "softer", high-nitrogen content diamonds that are less susceptible to fracture with uneven loads. The pressure gradient of the non-hydrostatic environment caused by diamond deformation is more evident than with low-nitrogen diamonds. On the other hand, these samples offer a view of material behavior under anisotropic pressure conditions potentially found at the reaction front of an explosive. We used high-nitrogen diamonds in these experiments to reduce cost and time-consuming diamond alignments between test shots.

Figure 1 shows the nitromethane data from Reference 1. The plot is annotated to illustrate the different reaction residues found in the DAC gaskets,[1] evolving with increasing pressure. Below 2 GPa gaseous products vent the gasket and leave a white solid. In the pressure range of 5-19 GPa the residue is black (soot), with inaudible venting of gaseous products above 15 GPa. Above 19-20 GPa there is almost no soot when the gasket vents and a clear residue when it remains intact. Above 25 GPa the gasket no longer vents gasses and the residue is clear and transparent, transforming to a white polycrystalline solid when pressure is released.

TATB

The burn rate for TATB was different from that of nitromethane in that it was slower and exhibited a distinct saw-tooth pattern with three burn rate maxima at ~18-, ~29- and ~39-GPa.[2] In the vicinity of each maximum is a transition region over which the color of the sample or products changes. These visual changes overlay published burn rate data in **Figure 2**, and briefly described in **Table 1**.

With TATB the most notable observation was the appearance of shiny polycrystalline zones or inclusions in the central highest-pressure regions of the sample. These zones had a metallic, mirror-like finish. A color gradient of dark to lighter red extended radially from these shiny zones. This color gradient appeared to match the expected pressure gradient across the face of the diamonds. When pressure was released, the sample returned to the original yellow but the zone remained distinguishable from the bulk. An example of TATB in the DAC loaded to 16.4 GPa is shown in **Figure 3**. As pressure increased the shiny zones encompassed an increasing fraction of the sample area. These zones exhibited a different compressibility with a ± 7-10% pressure gradient compared to the typical ± 5% seen for other materials in this DAC.

The reaction products did not always vent the gasket with increasing pressure. Above ~30 GPa, the residue was a translucent amber solid in which the ruby chips (used for pressure measurements) were clearly visible. The gasket hole was also smaller diameter than before ignition. In one example, residue with an unidentified chip of blue material left for three days in the DAC had transformed from clear to polycrystalline.

Shown in **Figure 4** is an example of residue from TATB that had been pre-loaded in the DAC to 31 GPa. We were unable to identify the solid residue by FTIR (Nicolet 60SX and IR PLAN microscope attachment) because of poor signal to noise due to the small sample size.

CL-20

We previously published work on the relative thermal stability[6,7] and the pressure-dependent burn rate[5] of the four well-defined polymorphs of CL-20 (α, β, γ, ε). We found that the epsilon (ε) polymorph to be the most thermodynamically stable phase, undergoing a phase transition to the gamma (γ) polymorph at 64 ± 1°C. [6]

Some of the large amount of burn rate data we collected is reproduced in **Figure 5**. The lines are guides to the eye to emphasize differences and commonalities among the polymorphs. All four polymorphs exhibit similar burn rate signatures up to ~8 GPa. Note the burn rate profiles of the α- and γ–polymorphs are almost identical up to ~20 GPa with a single line tracing through both sets of data. Over the range of 20-34 GPa the alpha sample follows the same pressure dependence as gamma but at a slower rate.

The most dramatic "saw tooth" burn rate behavior for each polymorph, not shown here, occurred at pressures >17 GPa with extreme swings between maxima to minima over small pressure increments. The fastest rates were ~1.2 km/s at 16-17 GPa for both the ε- and γ-polymorphs.

All samples remained colorless and transparent under pressure. Under 2 GPa, reactions were incomplete with as much as ~75% of the starting material left in the gasket. This residue contained soot-lined cracks propagating radially outward from the ignition

zone. If gaseous products were made at these low pressures they did not make an audible snap when breaking through the gasket.

Above 2 GPa, all the CL-20 polymorphs burned increasingly to completion with decreasing soot residue. Above 6-8 GPa, not only did samples burn to completion but also the product gases vented more forcefully with the rapidly increasing burn rate. There were no other observed changes to the reaction products up to the highest pressure attained (~40 GPa).

Along with the burn rate data we had previously obtained infrared spectra (Nicolet 730 FTIR) of each polymorph under static pressure to 13 GPa.[5] We examined two spectral regions in particular – that corresponding to the C-H stretch (3200-3000 cm^{-1}) and to the ring + NO_2 deformation modes (700 - 830 cm^{-1}). We observed monotonic changes in peak intensity, width, and frequency with increasing pressure occasionally interrupted by discontinuities, which along with other anomalies corresponded to abrupt changes in burn rate.

We found the γ-CL-20 polymorph to be extra sensitive to light when loaded to pressures ~8 GPa.[5] The samples accidentally ignited about 50% of the time with either the defocused backlighting Argon ion laser (514.5 nm, ~15 kW/cm^2) or the low power (<0.02 μJ) pulsed alignment laser. Because of this sensitivity, we were only able to measure the burn rate above and below ~8 GPa, as illustrated by the discontinuous line in **Figure 5.** Burn rate data for β-CL-20 was also difficult to measure at pressures > 8 GPa due to similar sensitivity to accidental ignition.

DISCUSSION

These three energetic materials demonstrate easily differentiated burn rate behaviors in the diamond anvil cell, from pressure dependence to maximum reaction rate from TATB (v_{max}~20 m/s at ~40 GPa) to CL-20 (v_{max}~1.2 km/s at ~17 GPa). There is some similarity in their reaction behavior because they share a common functionality, the nitramine group, which is the principle source of exothermic energy, permitting similar reaction pathways at low pressures. The trend for all three materials was to burn faster with increasing pressure, with transitions to different residue products corresponding to abrupt changes in burn rate. Soot is preferentially produced at the lower pressures, with a cut-off at ~8 GPa for CL-20 and ~20 GPa for NM and TATB. As pressure increases, intermolecular distances and molecular orientations change which preferentially opens up different reaction pathways for each material. CL-20 does not generate much soot, and achieved the highest burn rate. TATB produces more soot than nitromethane with a resultant slower maximum burn rate. Nevertheless, at the highest pressures studied, all three materials produced gaseous products, or a clear solid residue when confinement of the gasket remained intact.

The behavior of intra- and intermolecular bonds under increasing pressure creates a variable roadmap to energetically favorable reaction pathways in several ways. Under compression the crystal lattice distorts as the intermolecular distances decrease, often anisotropically. In response to further compression, molecules can twist and bend bonds to form a new polymorph (displacive transformation).[8] This change happens rapidly when a crystal structure enters the new P, T field of stability. Or the relative alignment of molecules can involve either intermolecular bond breakage or reorganization of molecules into a newly stable structure (reconstructive transformation). Either mechanism allows the

molecules to rearrange into a new packing arrangement within the crystal lattice. These transformations can be sluggish with the old polymorph persisting unstably even in the P, T field of the new phase. If the rate of transformation is slow under uniaxial shock conditions the availability of new reaction pathways will not be realized. However, other mechanisms such as shear may come into play under more realistic shock conditions that can facilitate an otherwise sluggish transformation.

Nitromethane

Recent work by others has investigated the structural and vibrational properties of solid nitromethane under high pressure,[9] as well as the effect of uniaxial strain up to 200 GPa on the band gap.[10] The latter work is noteworthy for their static calculations that show the C-H bond is highly stretched at a relatively early stage of uniaxial compression along the b lattice vector. They found that uniaxial compression did not cause a dramatic band-gap reduction associated with bending of the nitro group, and concluded that the onset for chemistry is strongly affected by pressure anisotropy.

With Raman spectroscopy, Courtecuisse et al.[11] proposed an estimate of the nitromethane phase diagram over the pressure range of 0-35 GPa to include three new low-temperature phases. According their phase diagram, a transition between chemical transformations between CII and transparent CI occurs at 11 GPa. Formation of the CI form from low-temperature phases is slow. Solid CI compound is recovered after releasing pressure at ambient pressure, but the Raman spectrum is indistinguishable from the ground state. While these observations appear consistent with this DAC work, the irreversible formation of CII, which is orange under white light transmission, does not appear to match our observations of NM since we saw no color changes under static pressure. They did not

see a Raman signal for the CII state that due to the small sample size. It is not clear how these as-yet unidentified forms of NM relate to the reaction chemistry of nitromethane under high pressure.

TATB

In our previous paper we discussed a number of different mechanisms to explain the change in color and appearance of shiny inclusions in TATB under pressure.[2] These included the possibility of phase transitions, formation of furoxan/furazan rings with exclusion of water, and realignment of the molecular rings with distortion of the crystal lattice under pressure and decrease intermolecular separation under compression.

Under ambient conditions, TATB molecules pack into graphitic layers of a triclinic lattice, the in-plane aromatic rings aligned with those in every other plane.[12] The inter- and intra-molecular hydrogen bond system between amine and adjacent nitro groups within each plane yields a structure tolerant of mechanical insult. Hydrogen bonding between donor hydrogen and acceptor atoms is a well-defined phenomenon, and is the dominant force behind the insensitivity of TATB.[13] Note that other less well-defined π-π aromatic interactions also play a role in how these molecules can pack into a crystal lattice.

According to the semiconductor model of explosive initiation, the electrical conductivity of TATB is expected to sharply increase to values typical of semiconductors under conditions of shock wave compression.[14] The assumption is a combustion wave propagates from "hot-spot" microsites by means of electron heat conduction. For TATB, the energy gap is predicted to be $\varepsilon_g = 1.5\text{-}2.0$ eV in the pressure range of 10-20 GPa, which

is close to the detonation threshold.[14] It is notable that the shiny inclusions appearing ~18 ± 2 GPa, may be a visual indicator of metallization in agreement with this theory.

Other studies have theoretically assessed the possible role of pressure-induced metallization in TATB. Wu et al.[15] compressed the crystal perpendicular to the TATB molecular sheet since it was believed to be the easiest direction to induce metallization. They found that band-gap closure begins near 47% uniaxial strain, with a lower pressure bound for metallization of ~120 GPa, far above the detonation pressure of TATB. A later study by Zhang et al.[16] of the crystalline structure of TATB concluded that the crystal exists as a semiconductor at 0.1-100 GPa with a predicted transition to conductor at hundreds of GPa. Neither study would appear to shed light on the visible changes seen in TATB under high pressure in the DAC.

While the semiconductor theory would predict onset for metallization where we first observe shiny inclusions in TATB in the DAC, it of course does not predict behavior at higher pressures above shock initiation. In order to explain behavior at higher pressure, we propose a collapse of the graphitic layers to one or more herringbone motifs commonly found among aromatic hydrocarbon molecules.

The packing patterns of geometrically similar planar aromatic hydrocarbons were studied by Gavezzotti et al.,[17] They found that there are only a small number of well-defined ways these molecules pack into a crystal lattice: herringbone, sandwich-herringbone, sandwich-herringbone β, and sandwich-herringbone γ. These types differ mainly with respect to the relative orientation of molecular planes in the crystal, which is reflected in the length of the shortest cell axis. The simplest packing is the herringbone in

which the molecules form stacks aligned edge-to-face with neighboring stacks. The sandwich herringbone is made up of pairs of parallel molecules. The γ packing is described as a sort of flattened herringbone. Lastly the β motif is a layered structure made up of graphitic planes - the TATB crystal structure falls into this category.

The interplanar distance of molecules is not infinitely compressible. If the first burn rate maximum at ~18 GPa is the alignment of aromatic rings in neighboring planes, maxima at 31- and 39-GPa could correspond to other polymorphic phase changes. One possibility includes the transition to different herringbone packings. In his study of planar aromatic compounds, Gavezzotti[17b] was able to group the different structures by the shortest lattice cell axis. The β herringbone (e.g. TATB) typically had the shortest axis, while the next shortest is the γ herringbone. To transition from graphitic to γ-herringbone would liberate previously H-bonded amine and nitro groups. Formation of highly oxygenated compounds like dinitrogen trioxide,[18] which is a blue solid, and furoxan/furazan rungs could become favorable reaction pathways.

Other small highly–colored molecules exist at high pressure but do not match our observations in the relevant pressure regime. For example, at room temperature oxygen turns from a light-blue solid to orange at the β- to δ-O_2 transition (~5 GPa) then to red at the δ- to ε-O_2 transition (~10 GPa).[19] So the blue high-pressure inclusions we see in residue >17 GPa cannot be oxygen, however intriguing the idea. Nevertheless the deepening red of oxygen with increasing pressure, indicative of strong intermolecular interactions between O_2 molecules (O_4 clusters),[20] is similar to the deepening red of TATB. These parallel observations suggest that similar interactions between nitro groups may be taking place

should the intermolecular hydrogen-bonding network of the herringbone-packed TATB molecules be interrupted (e.g. phase transition).

CL-20

The burn rate behavior of CL-20 polymorphs indicates that spatial orientation of reactive groups about the rigid cage dominates chemical reaction pathways at least initially for lower pressures studied. The basic structure of CL-20 is a rigid isowurtzitane cage with a nitro group attached to each of the six bridging nitrogens within the cage (**Figure 6**).[21] These nitramine appendages are flexible - the amine nitrogen can convert from a planar to a pyramidal conformation with little energy. We number nitrogens in the cage to identify the different possible conformers.[6] Each polymorph is distinguished by the endo-exo orientation of nitro groups about the six- and five-member rings of the cage and differences in crystal structure. The four identified polymorphs typically studied display only three conformations - the $\alpha-$ and $\gamma-$forms are essentially the same conformation but with different crystal packing and densities.

There are a number of possible polymorphs based on molecular conformation that have yet to be identified. **Table 2** is simplified table of CL-20 conformational polymorphs discussed in Reference 6. Each set of four exo/endo orientations of the NO_2 groups with respect to the two 5-membered rings (left column) can theoretically have up to four different exo/endo orientations of the NO_2 groups on the 6-membered ring. A dash indicates a redundant structure. The "N" designator indicates that bending both the NO_2 groups into the crowded endo-endo configuration would be unstable. In addition to the four additional conformers predicted to be sterically stable (*) are five more we consider possible but less likely due to crowding of the nitro groups.

The near perfect match of the pressure-dependent burn rate of identical α- and γ-conformers neatly illustrates that packing in the crystal lattice has little effect on reaction chemistry, especially since α-CL-20 usually exists as a hydrate. Using this analogy, the concurrent dips in burn rate of β-and ε-polymorphs at 2 GPa and 4.5 GPa suggests that the one nitramine orientation in common (N-8) is being affected by pressure, not the N-10 or N-4 groups on the 6-memberd ring. These transitions correspond to β → "New 1" and ε → "New 2" respectively. Thereafter the behavior of these two polymorphs diverge as the β-phase passes through an anomalously light-sensitive transition region ~8 GPa. This behavior could indicate rotation of a nitro group causing more internal ring strain. One possible transition could be "New 1" → "New 3," the same 6-membered ring involved as the first transition. Another possibility is the "New 1" → "New 4" transition which forces the last nitro group into a highly symmetric but sterically hindered configuration.

CONCLUSIONS AND SUMMARY

When molecular reorientation, alignment or repacking occurs, formerly energetically favorable reaction pathways can become less favorable, resulting in different reaction rates and products. These changes can also affect sensitivity to external insults, whether mechanical (shock, impact), friction, or electronic (static, electromagnetic). Clearly the role of functional group interactions between neighboring molecules plays a role in determining initial reaction pathways.

This work provides more information to shed light onto high-pressure reaction chemistry of energetic materials. We believe it shows that not realignment of molecules within the crystal lattice but also more subtle reorientation of functional groups can make

significant changes to available reaction pathways under anisotropic pressure conditions similar to that found at the reaction front of explosives.

REFERENCES

1. Rice, S.R., Foltz, M.F., "Very High Pressure Combustion: Reaction Propagation Rates of Nitromethane within a Diamond Anvil Cell," *Combustion and Flame*, Vol. 87, pp. 109-122, 1991.

2. Foltz, M.F., "Pressure Dependence of the Reaction Rate of TATB at High Pressure," *Propellants, Explosives, Pyrotechnics,* Vol. 18, pp. 210-216, 1993.

3. Foltz, M.F., "Pressure Dependence on the Reaction Propagation Rate of PETN at High Pressure," *Proceedings of the 10th Detonation Symposium*, pp. 579-585, Boston, MA, July 1993.

4. Foltz, M.F., Maienschein, J.L., "Ammonium Perchlorate Phase Transitions to 26 GPa and 700 K in a Diamond Anvil Cell," *Materials Letters*, Vol. 24, pp. 407-414 (1995).

5. Foltz, M.F., "High Pressure Combustion of CL-20 Polymorphs in a Diamond Anvil Cell," *1991 JANNAF CL-20 Symposium*, China Lake, CA, May 1991.

6. Foltz, M.F., Coon, C.L., Garcia, F., Nichols III, A.L., "The Thermal Stability of the Polymorphs of Hexanitrohexaazaisowurtzitane, Part I," *Propellants, Explosives, Pyrotechnics,* Vol. 19, pp. 19-25 (1994).

7. Foltz, M.F., Goon, C.L., Garcia, F., Nichols III, A.L., "The Thermal Stability of the Polymorphs of Hexanitrohexaazaisowurtzitane, Part II," *Propellants, Explosives, Pyrotechnics,* Vol. 19, pp. 133-144 (1994).

8. Bloss, F.D., "Structural Variations, Composition, and Stability," in *Crystallography and Crystal Symmetry*, pp. 318-320, Holt, Rinehart and Winston, New York, 1971.

9. Liu, H., Zhao, J., Wei, D., Gong, Z., "Structural and vibrational properties of solid nitromethane under high pressure by density functional theory," *Journal of Chemical Physics*, 124(12), 124501, 2006.

10. Margetis, D., Kaxiras, E., Elstner, M., Frauenheim, Th., Manaa, M.R., "Electronic structure of solid nitromethane: Effects of high pressure and molecular vacancies*," Journal of Chemical Physics,* 117(2), pp. 788-799, 2002.

11. Courtecuisse, S., Cansell, F., Fabre, D., Petitet, J.-P., "Phase transitions and chemical transformations of nitromethane up to 350 °C and 35 GPa*," Journal of Chemical Physics,* 102(2), pp. 968-974, 1995.

12. Cady, H.H., Larson, A.C., "The Crystal Structure of 1,3,5-Triamino-2,4,6-trinitrobenzene," *Acta Crystallographica,* 18, pp. 485-496, 1965.

13. Kolb, J.R., Rizzo, H.F., "Growth of 1,3,5-Triamino-2,4,6-trinitrobenzene (TATB) I. Anisotropic Thermal Expansion*," Propellants and Explosives*, 4, pp. 10-16, 1979.

14. Grebenkin, K.F., Zherebstov, A.L., Kutepov, A.L., Popova, V.V., "On the Experimental Verification of the Semiconductor Model of Detonation," *Technical Physics,* 47 (11), 1458-1460, 2002.

15. Wu, C.J., Yang, L.H., Fried, L.E., Quenneville, J., Martinez, T.J., "Electronic structure of solid 1,3,5-triamino-2,4,6-trinitrobenzene under uniaxial compression: Possible role of pressure-induced metallization in energetic materials," *Physical Review B*, 67, pp. 235101, 2003.

16. Zhang, C., Shu, Y., Zhao, X., Wang, X., "Theoretical Study on Crystalline Structures of TATB at Different Pressures," *Science and Technology of Energetic Materials*, 66(2), pp. 261-265, 2005

17.a. Desiraju, G.R., Gavezzotti, A., "From Molecular to Crystal Structure; Polynuclear Aromatic Hydrocarbons," *Journal of the Chemical Society - Chemical Communications*, 10, pp. 621-623, 1989; b. Desiraju, G.R., Gavezzotti, A., "Crystal Structures of Polynuclear Aromatic Hydrocarbons. Classification, Rationalization and Prediction from Molecular Structure," *Acta Crystallographica,* B45, pp. 473-482, 1989.

18. Wang, X., Qin, Q.-Z., "A new conformer of dinitrogen trioxide in low temperature matrix: trans-cis N_2O_3," *Spectrochimica Acta Part A,* 54, pp. 575-580, 1998.

19. Desgreniers, S., Vohra, Y.K., Ruoff, A.L., "Optical Response of Very High Density Solid Oxygen to 132 GPa," *Journal of Physical Chemistry*, 94, pp. 1117-1122, 1990.

20. Santoro, M., Gregoryanz, E., Mao, H.-k., Hemley, R.J., "New Phase Diagram of Oxygen at High Pressures and Temperatures*," Physical Review Letters*, 93, pp. 265701, 2004.

21. Gilardi, R., "Polytypical Polymorphs Occurring in an Energetic Material," *Virtual Course on Polymorphism: Diversity Amidst Similarity*, International School of Crystallography, Erice, Italy (June 2004).

Table 1. Pressure-dependent changes observed in TATB

Pressure (GPa)	Visual Observation	Burn Rate Behavior
~2.6 to 18	Increasingly colored, tinting from yellow to red.	Monotonically increasing burn rate and less soot residue.
~17 to 20	First see shiny (reflective) inclusions in high-pressure region.	Maximum then abrupt change to slower rate.
~18 to 28	Sample is red with shiny inclusions in the high-pressure region.	Monotonically increasing burn rate with no soot residue.
~27.6 to 31	No new color changes in the sample.	Maximum then abrupt change to slower burn rate. When gasket doesn't vent, an amber residue is left behind.
~30 to 37	Dark, opaque red zones surround the now highly reflective (mirror-like) inclusions in the high-pressure region.	Monotonically increasing rate.
~37 to 41	No new color changes in the sample.	Maximum then abrupt change to slower rate. When the gasket vents, no residue. When gasket doesn't vent, the residue is an amber polycrystalline material with light blue chips.

Table 2. Top views of the conformers of CL-20 (from Reference 6)

| Structure | Polymorph (N-10) - (N-4) Orientation | | | |
	exo-exo	exo-endo	endo-exo	endo-endo
	α * γ *	Y *	Y *	N
	β *	Y *	—	N
	Y *	ε *	—	N
	New 3 Y *	Y	Y *	N
	New 1 Y *	New 2 Y *	Y	N
	New 4 Y	Y	—	N
	Y *	Y	—	N
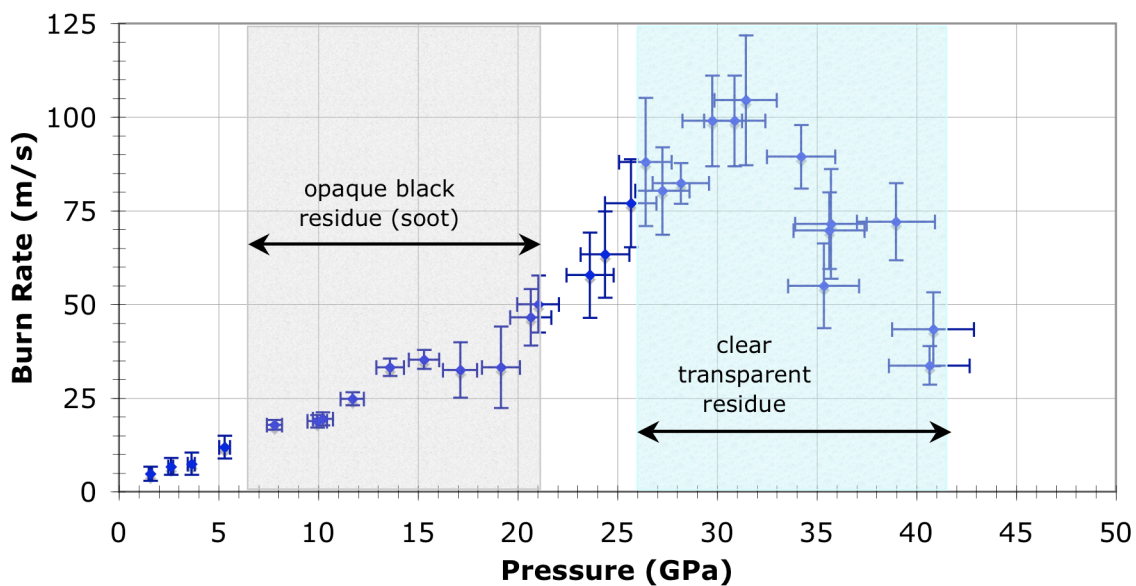
Figure 1. NM burn rate with observed changes in the reaction products (Ref. 1).
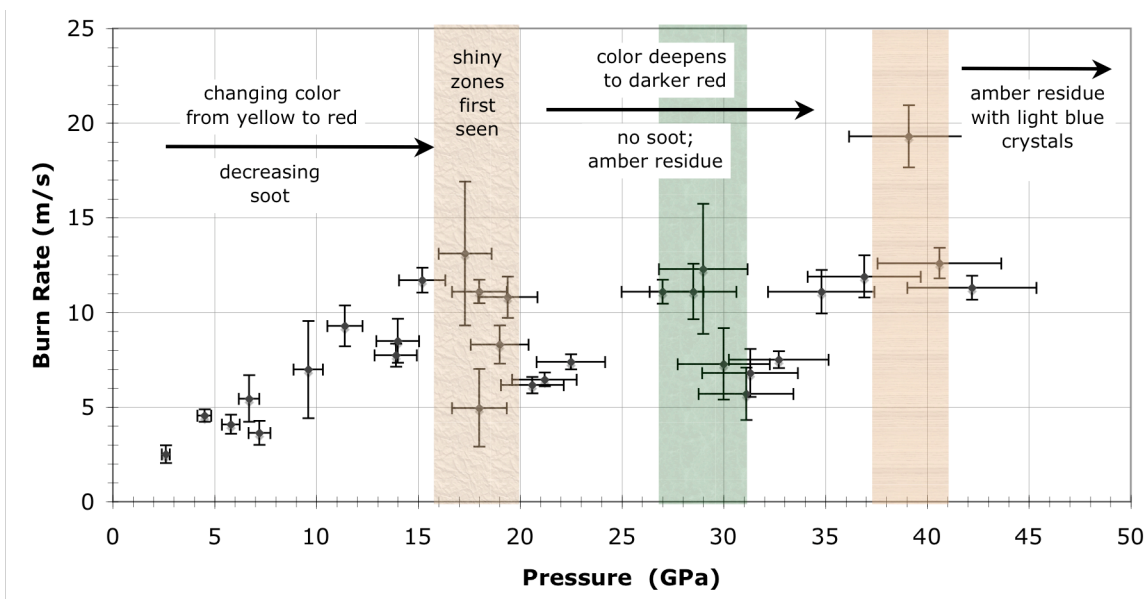
Figure 2. TATB burn rate and observed changes to the sample and residue.
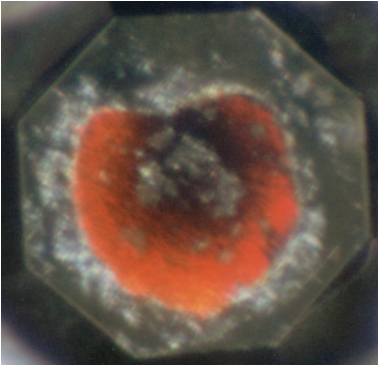
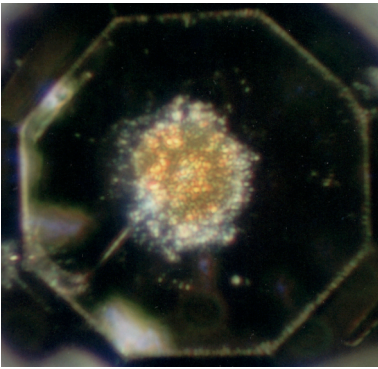**Figure 3. TATB pressurized to 16.4 GPa.**

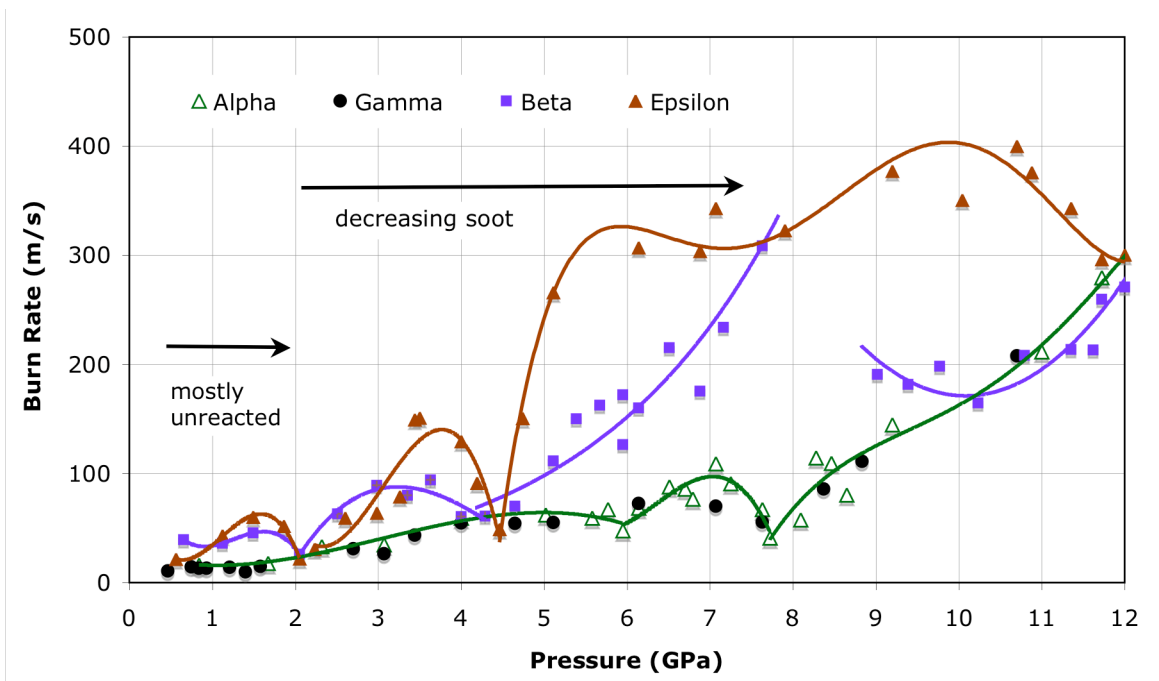**Figure 4. Amber and pale blue residue from TATB loaded to 31 GPa.**

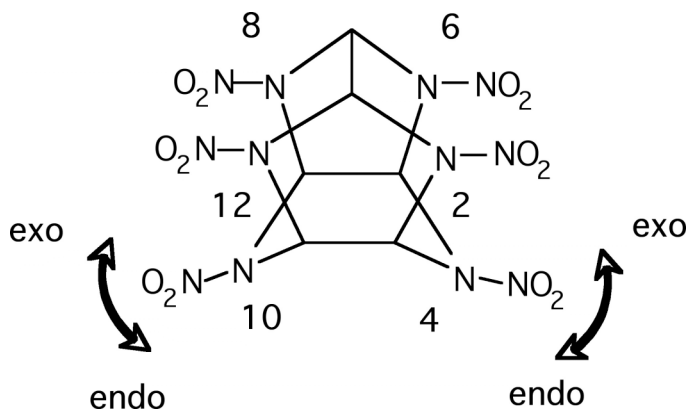**Figure 5. Pressure-dependent DAC burn rate of four CL-20 polymorphs.**

Figure 6. Numbering of CL-20 nitramine orientations for conformers in Table 2.